RESEARCH

Studies of the low- and high-order optical nonlinearities of mercury selenide quantum dots using femtosecond pulses

G. S. Boltaev[1,2,3] · R. A. Ganeev[2,3,4,5] · I. A. Shuklov[6] · A. A. Lizunova[6] · D. V. Dyomkin[6] · T. Milenkovich[6] · A. Abu Baker[1] · A. S. Alnaser[1]

Abstract

The nonlinear optical properties of the synthesized mercury selenide quantum dots (HgSe QDs) were investigated using near-infrared femtosecond pulses (1030 nm, 40 fs). The two-photon absorption in the HgSe QD suspension was analyzed. The third-harmonic generation was studied using the 70-nm-thick HgSe QDs film. The high-order harmonics generation up to the 37th order in the laser-induced plasmas containing HgSe QDs was demonstrated.

1 Introduction

The narrow band gap quantum dots (QD) can be used for different applications such as synthesizers, biomarkers, plasmonic luminescence imaging, etc. [1–4]. Alongside the optical properties, various metal-alloy QDs have recently demonstrated advanced nonlinear optical properties, which can be used in optoelectronics, optical limiting of radiation, and for laser mode-locking and Q-switching [5, 6].

The majority of the nonlinear optical studies of QD-containing materials were carried out at the conditions when the small-sized species were presented in the colloidal suspensions. In the meantime, the application of thin films and

✉ R. A. Ganeev
rashid.ganeev@lu.lv

✉ I. A. Shuklov
shuklov.ia@mipt.ru

[1] Department of Physics, American University of Sharjah, Sharjah 26666, UAE

[2] Institute of Fundamental and Applied Research, TIIAME National Research University, Kori Niyozov Str. 39, 100000 Tashkent, Uzbekistan

[3] Chirchik State Pedagogical University, 104 Amir Temur, 111700 Chirchik, Uzbekistan

[4] Laboratory of Nonlinear Optics, University of Latvia, Jelgavas 3, Riga 1004, Latvia

[5] Department of Physics, Voronezh State University, Voronezh 394006, Russia

[6] Moscow Institute of Physics and Technology (National Research University), Dolgoprudny 141701, Russia

laser-induced plasmas (LIP) containing such QDs can further exploit their unique quantum confinement-related properties. These effects have been, particularly, demonstrated in the case of HgTe QD thin films in the UV, Visible, and near-infrared ranges using tunable femtosecond pulses [7].

Among various QDs, the mercury selenide (HgSe) QDs also have potential applications in various areas [8]. The narrow band gap energy of HgSe QDs makes them useful optical materials in the infrared spectral range [9]. In [10], HgSe nanocrystals were synthesized from selenourea and mercury chloride in oleylamine. The theoretical analysis confirmed that the combination of a stoichiometric HgSe nanocrystal and alkylammonium chloride ligands forms a stable structure. In the review of Green and Mirzai [11], synthetic chemistry has been explored behind the preparation of HgSe QDs. They highlighted the synthetic chemical routes to nanostructures of mercury chalcogenides, particularly HgSe, and their promising optical characteristics across the visible and near-infrared regions, offering alternatives to typical III–V and IV–VI-based QDs. A new generation of colloidal QD-based photodetectors, which demonstrated the sensitivity improved by 2 orders of magnitude and the optical absorption that can be continuously tuned between 3 and 20 µm, was reported in [12]. These photodetectors are based on the synthesis of n-doped colloidal HgSe QDs whose sizes can be tuned continuously between 5 and 40 nm, and on their assembly into the solid nanocrystal films.

HgSe QDs can be used for the optical limiting and high-order harmonics generation (HHG) of ultrashort laser pulses, similar to the metal sulfide-containing QDs [13]. Earlier, the low-order optical nonlinearities of colloidal HgSe QDs

in the visible and near-infrared ranges were studied using the long (10 ns) probe pulses [14]. The application of femtosecond pulses can further amend the knowledge about the ultrafast nonlinear optical processes in HgSe QDs.

In this paper, the results of studies of the low-order nonlinear optical properties of HgSe QD suspensions and thin films are presented. We also demonstrate the HHG in the LIP containing these QDs. We analyze the two-photon absorption (2PA) of the suspension containing these QDs. The 70-nm-thick films containing HgSe QDs were used for the third-harmonic generation (THG) of 1030 nm pulses. The LIP produced on the surface of HgSe QDs film was used as a nonlinear medium for the generation of high-order harmonics.

2 Synthesis and characterization of HgSe QDs

The physical properties of colloidal nanomaterials like HgSe QDs depend on their chemical composition. The material of the semiconductor core and Hg:Se ratio influences the

properties of HgSe QDs. These properties also depend on the used materials, preparation, and work-up procedure. The surfactants and solvents used during the synthesis also affect the morphology and optical characteristics of obtained nanocrystals.

The synthesis and characterization of HgSe QDs were similar to the one described in [14]. The morphological and optical characteristics of synthesized HgSe QDs showed similarities with those reported in [12]. The mean particle sizes and particle size distribution of synthesized HgSe QDs were investigated by a transmission electron microscope (TEM, JEM-2100, JEOL). The well-formed nanocrystals of spherical shape with a mean diameter of 7.5 nm were obtained at 100 °C (Fig. 1a, b). The optical properties were analyzed by a UV–Vis-NIR spectrophotometer (V-770, JASCO). The absorption measurements of the synthesized HgSe QDs showed a weak absorption peak at 1210 nm (Fig. 1c), which was attributed to the interband transition. The absorption peak in the mid-IR range with the maximum at 3950 nm was attributed to the intraband transition (Fig. 1d).

The thin films of HgSe QDs were prepared using the obtained colloidal solutions. The film's thickness was
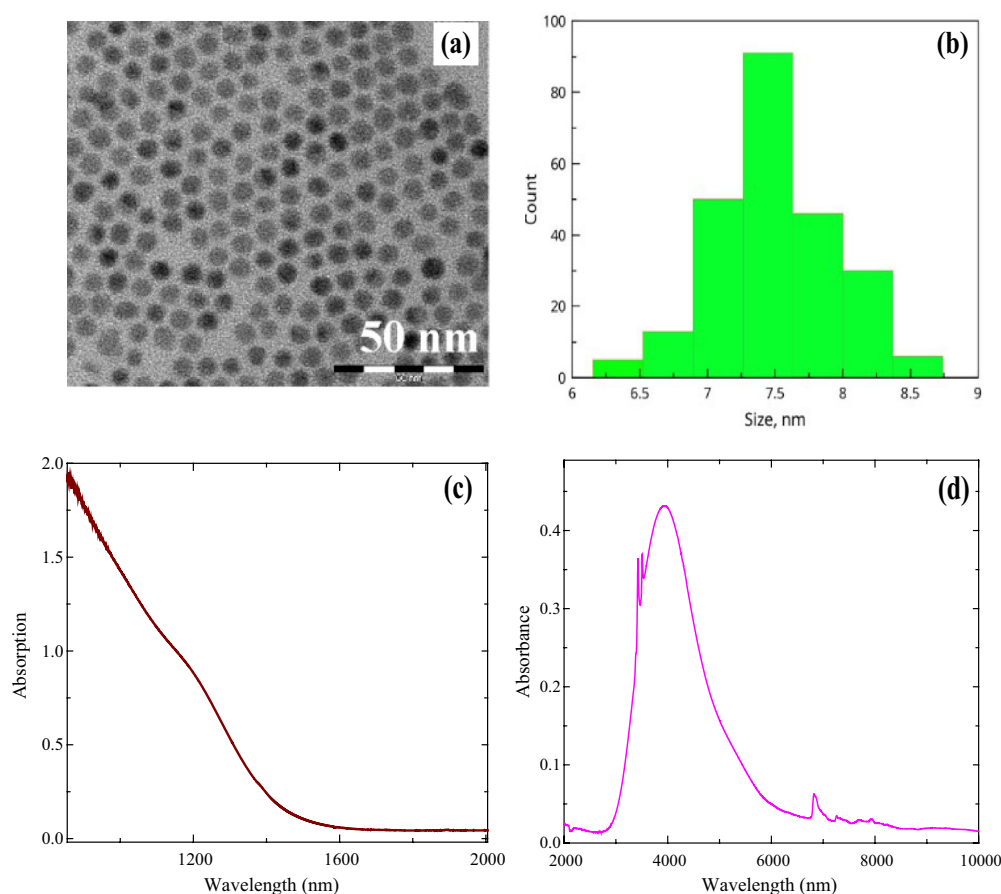
Fig. 1 **a** TEM of HgSe colloidal QDs. **b** Size distribution of HgSe QDs. **c** The absorption spectrum of HgSe colloidal QDs at the 850–2000 nm spectral range. **d** The absorption spectrum of HgSe colloidal QDs at the 2000–10,000 nm range.

qualitatively controlled by the number of drops used for the deposition of the suspension on the substrate. We further characterized the thickness of deposited films by the following method. The coating was scratched to analyze the thickness of the films. The atomic force microscope was used for the analysis of the scratches, which allowed for the determination of the 60–100 nm thickness for different samples. In our THG experiments, we used the 70-nm-thick films of HgSe QDs. Much thicker films (500 nm) were prepared for the ablation and formation of the HgSe QDs plasma. The thickness of the sample played an important role in creating the plasma containing a sufficient amount of quantum dots.

3 Experimental setups for the nonlinear optical studies of HgSe QDs

The formation of the thin (70 nm) film containing these QDs on the fused silica plate allowed for investigating the THG during the propagation of femtosecond pulses through these films. For HHG, the LIP was formed using the ablation of the thick (500 nm) films containing HgSe QDs. The plasma formation on the surface of these films was performed by using the heating laser pulses.

The Yb-doped fiber laser (UFFL_300_2000_1030_300; Active Fiber System) was used in these studies. The standard Z-scan technique was used for the analysis of the low-order nonlinearities of studied suspensions and films. The fundamental radiation ($\lambda = 1030$ nm, pulse duration 40 fs, pulse repetition rate 50 kHz) was focused using a 400 mm focal length spherical lens (Fig. 2a). The beam waist diameter was 60 μm. The intensity of the probe pulse was equal to 2×10^{11} W cm^{-2}. We diluted the HgSe QDs solution by mixing 2 ml HgSe QDs solvent and 5 ml *n*-hexane solution. This solution was inserted in the 1 mm thick silica glass cells for further measurements of the nonlinear optical processes in HgSe QDs.

The HHG setup is shown in Fig. 2b. The energy of the 40 fs driving pulses (DP) was kept at 0.7 mJ, while the energy of the uncompressed 240 ps heating pulses (HP) was 1 mJ. The used intensity of the 40 fs DP focused in the plasma area was $I_{DP} \approx 2 \times 10^{14}$ W cm^{-2}. We used the uncompressed 240 ps pulses from the same laser to ablate the 500-nm-thick film comprising HgSe QDs. The intensity of the focused HP on the surface of the film was $\sim 4 \times 10^{11}$ W cm^{-2}. The delay between HP and DP was ~ 70 ns. This delay was maintained by using the optical path difference between HP and DP pulses. The high-order harmonics and laser-induced emission of plasma were analyzed using an extreme ultraviolet (XUV) spectrometer (HP Spectroscopy GmbH, Germany) consisting of a gold-coated cylindrical mirror, flat-field grating, microchannel plate with phosphor screen, and CCD camera.

(a)

(b)
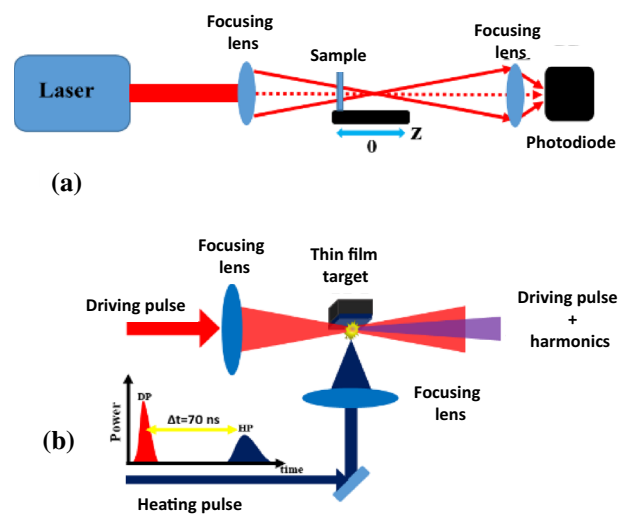
Fig. 2 **a** Experimental scheme for Z-scan measurements. **b** Experimental scheme for HHG in HgSe QDs plasma. The delay between heating and driving pulses was 70 ns

4 Results

To analyze the nonlinear absorptive properties of materials, a Z-scan technique was used. The open-aperture (OA) Z-scan scheme allowed for analyzing the dependence of the sample transmittance on its position in the vicinity of the focal plane of the focusing lens. The positive nonlinear absorption was observed during OA Z-scan measurements. Meanwhile, the closed-aperture Z-scan study did not reveal the nonlinear refraction in the HgSe QDs suspension. The application of long (10 ns) pulses has earlier demonstrated the negative nonlinear refraction of HgSe QDs, which was attributed to the thermal-related process and/or molecular Kerr effect [14]. In our case (40 fs probe pulses), the most probable mechanism could be the electronic Kerr-related refractive nonlinearity. However, this process was not observed during these studies.

The OA Z-scan curve of a normalized transmittance was recorded during the scanning of the sample along the z-axis of the focused laser beam. Figure 3a shows the normalized transmittance of the HgSe QDs suspension. We used the relation [15] to fit the OA data and determine the nonlinear absorption coefficient (β) responsible for 2PA:

$$T \approx 1 - q(z)/2(2)^{1/2}. \tag{1}$$

Here $q(z) = \beta I_0 L_{eff}/[1 + (z/z_0)^2]$, $z_0 = k(w_0)^2/2$ is a Rayleigh length, $k = 2\pi/\lambda$ is a wave number, w_0 is a beam waist radius at the $1/e^2$ level of intensity distribution, I_0 is an intensity in the focal plane, $L_{eff} = [1 - \exp(-\alpha_0 L)]/\alpha_0$ is an effective length of the medium, α_0 is a linear absorption coefficient, and L is the thickness of the sample. The value of
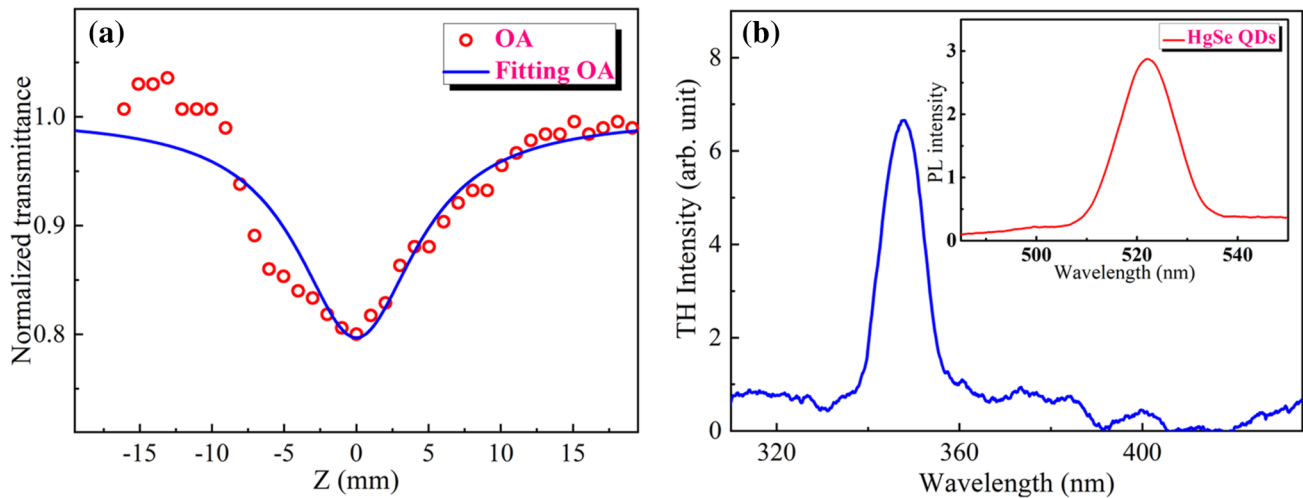
Fig. 3 **a** Open-aperture Z-scan measurement of the HgSe QD suspension inserted in the 1 mm thick fused silica cell. **b** THG spectrum generated in a thin film using the 1030 nm driving laser pulses. Inset: two-photon photoluminescence spectrum (peak at the wavelength of 522 nm) of the HgSe QD thin film.

the nonlinear absorption coefficient of the HgSe QDs suspension at the 1030 nm wavelength was calculated to be $\beta = 3 \times 10^{-9}$ cm W^{-1}.

We also carried out the THG and photoluminescence (PL) studies using the thin film containing HgSe QDs. The HgSe QDs were deposited gradually on a 0.8 mm thick fused silica substrate via a layer-by-layer technique [16]. This process was repeated five times. The thickness of the used film was 70 nm. The spectrum of the generated third harmonic is shown in Fig. 3b. The frequency up-conversion of femtosecond near-IR laser pulses allowed for the generation of the third-harmonic emission at the wavelength of 343 nm. The THG conversion efficiency was estimated to be 10^{-5}.

The PL spectrum is shown in the inset in Fig. 3b. The nature of two-photon excited luminescence is an excitation of electrons from the ground state to the excited state of QDs due to the intraband transition of free carriers in the field of the laser pulse [17]. The PL was detected by a spectro-photometer with 300 μs integration time at the 400–600 nm spectral range. In the case of two-photon excitation, the PL peak of the HgSe QDs corresponded to the visible range ($\lambda = 522$ nm, inset in Fig. 3b).

During the ablation of QD-containing film, the probability of the interaction of strong laser fields with multi-atomic QDs is possible thus allowing the generation of efficient high-order harmonics compared with the single-atom species. The multi-atomic metallic nanoparticles [18, 19], molecular QDs [20, 21], and gas clusters [22, 23] became attractive media for the generation of coherent XUV radiation through HHG. At the high intensity of DP ($I_{DP} > 1 \times 10^{14}$ W cm^{-2}), the generation of high-order harmonics in the LIP containing small-sized QDs is possible.

The ablation of the thick film containing QDs during our studies was performed using the heating laser beam (4×10^{12} W cm^{-2}). The variation of the intensity of heating laser pulses allowed optimizing the conditions of the LIP for efficient HHG in the case of a high-pulse repetition laser (50 kHz). Previously, the dependence of harmonic yield on the energy of heating laser pulses was analyzed [24] and the harmonics generation in plasma using a high-pulse repetition rate laser was reported [25].

Figure 4a presents the raw images of the harmonics generated in the LIPs containing HgSe QDs (upper panel) and carbon atoms and ions (bottom panel). In the case of carbon LIPs, we observed relatively strong HHG due to the formation of the optimal plasma on the surface of bulk graphite. Notice that the concentration of carbon plasma was notably larger than the one of QD LIP, which led to a larger harmonic yield in the case of the former species. Figure 4b shows the line-out of the high-order harmonics generated in the LIP containing HgSe QDs. The HHG conversion efficiency in the plateau region was estimated to be 10^{-7}. During these studies, the high-order harmonics up to the 37th order were observed.

The mechanism of HHG in QDs is similar to the same process in gases [26]. Following this model, the harmonics generation results from the tunneling ionization, acceleration, and recombination of the ejected electron from the atoms assembled in the quantum dots. In the present study, we analyzed the spectrum of the harmonics generated in the plasma containing HgSe QDs, which was formed during the laser ablation of the 500 nm film. The substrate (0.5 mm thick silica glass plate) did not play a significant role in HHG since it was not ablated at the used fluence of the heating pulses and did not form the plasma containing the components of silicon oxide.
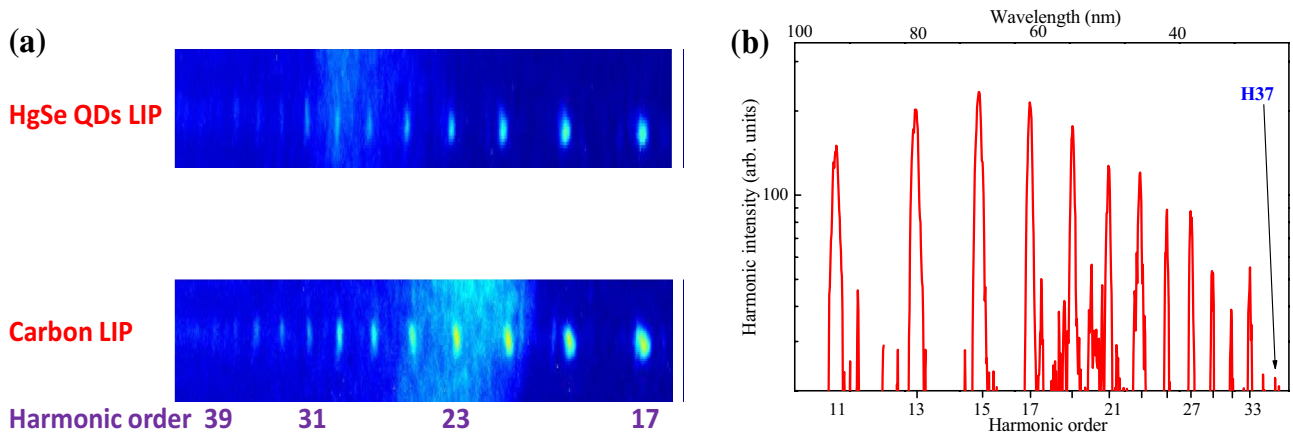
Fig. 4 a Raw images of the harmonic spectra generated from HgSe QD plasma (upper panel) and carbon plasma (bottom panel). The bottom axis shows the order of harmonics. **b** The line-out of the harmonic spectrum generated in the LIP containing HgSe QDs

5 Novelties of study

The major topic of this research is the nonlinear optical study of synthesized QDs. Notice that the synthesis of HgSe QDs described in this manuscript has been demonstrated in a few previous reports [12, 14]. Here, we address the comparison between the studies of HgSe QDs using the pulses of different duration. In the case of nanosecond pulses, the negative nonlinear refraction of HgSe QD suspension, which was attributed to the orientational Kerr effect rather than thermal lens formation, has been reported in [14]. The value of the nonlinear refractive index was determined to be $\gamma = -5 \times 10^{-12}$ cm^2 W^{-1}. Our present studies using femtosecond pulses did not reveal this process in the studied suspension since the electronic Kerr effect is weaker than the orientational molecular Kerr effect in the case of the molecular structures. Meanwhile, the nonlinear absorption was observed in two cases (i.e., using nanosecond and femtosecond probe pulses). The nonlinear absorption coefficient ($\beta = 9 \times 10^{-7}$ cm W^{-1}) of those colloidal quantum dots determined using nanosecond pulses ($\lambda = 532$ nm, [14]) was more than two orders of magnitude larger compared with the present studies using the 1030 nm, 40 fs pulses ($\beta = 3 \times 10^{-9}$ cm W^{-1}).

A significant difference in the nonlinear absorption coefficients in these two studies is related to the application of the notably shorter wavelength (532 nm) radiation in the case of nanosecond pulses. The two-photon absorption, in that case, is significantly larger compared with the same process using the longer wavelength pulses (1030 nm).

Another novelty of present studies is a generation of high-order harmonics in the plasmas containing HgSe QDs using the new approach in the formation of the QDs-containing plasma. Previously, HHG in QDs has been reported in a few studies [13, 27]. Those studies reported the properties of the QDs of metal sulfides (CdS, Ag$_2$S, and ZnS). The laser plasma in those cases was produced on the surfaces of the mixtures of QDs and gelatin, which made it difficult to distinguish the relative role of the later species (gelatin) in harmonics generation compared with the QDs. In the present case, we used another technique to exclude the influence of the component (gelatin), which played the role of glue in previous studies [13, 27] to maintain the QDs in a solid form for laser ablation. The HgSe QD-containing film was ablated to form the LIP containing only QDs. Correspondingly, in that case, the only species responsible for the generation of high-order harmonics are the HgSe QDs.

The third novelty is the application of the HgSe multiparticle species as the sources of harmonics, contrary to the abovementioned use of metal sulfide QDs. The advantages of the former QDs are the formation of relatively thick films for further laser ablation. In previous cases (CdS, Ag$_2$S, and ZnS QDs), the difficulties in the deposition of the thick layers of metal sulfide QDs on the substrates prevented carrying out the ablation and formation of the QD-containing plasmas of sufficient density allowing observation of harmonics.

The additional advantages in the application of the HgSe QDs as the emitters of high-order harmonics are as follow.

Contrary to other similar experiments with metal sulfide QDs, the mercury selenide quantum dots demonstrated better stability of the harmonics generation, larger harmonic cutoff, and larger yield of coherent short-wavelength radiation, as well as rather "clean" conditions for QD plasma formation using the ablation of the relatively thick films dominantly containing HgSe QDs.

6 Conclusions

We have reported the nonlinear optical studies of HgSe QD films and suspensions. The two-photon absorption of QD suspension ($\beta = 3 \times 10^{-9}$ cm W^{-1}) was analyzed in the case of 1030 nm, 40 fs probe pulses. Third-harmonic generation was demonstrated during the propagation of the femtosecond pulses through the 70-nm-thick HgSe QD film. High-order harmonics up to the 37th order were generated in the plasmas containing HgSe QDs. Our studies have demonstrated that HgSe QD thin films and suspensions can be used for optical limiting and low-order harmonics generation. The optimal ablation of films allowed for the formation of the plasmas that are suitable for producing coherent XUV radiation through the high-order harmonics generation.

Summing up, the advantage of HgSe QDs is mostly underlined from the point of view of their application in HHG. Correspondingly, one can consider those QDs as advanced materials from the point of view of their high-order nonlinear optical properties.

Declarations

Conflict of interest The authors declare no conflicts of interest.

References

1. T. Frecker, D. Bailey, X. Arzeta-Ferrer, J. McBride, S.J. Rosenthal, ESC J. Solid State Sci. Technol. **5**, R3019–R3031 (2016)
2. W. Sukkabot, J. Computat, Electronics **15**, 756–762 (2016)
3. G. Shen, P. Guyot-Sionnest, J. Phys. Chem. C **120**, 11744–11753 (2016)
4. D.R. Larson, W.R. Zipfel, R.M. Williams, S.W. Clark, M.P. Bruchez, F.W. Wise, W.W. Webb, Science **300**(5624), 1434–1436 (2003)
5. I.D. Skurlov, E.A. Ponomareva, A.O. Ismagilov, S.E. Putilin, I.A. Vovk, A.V. Sokolova, A.N. Tcypkin, A.P. Litvin, Photonics **7**, 39 (2020)
6. M. Yan, W.-D. Yao, W. Liu, R.-L. Tang, S.-P. Guo, Inorg. Chem. **60**, 16917–16921 (2021)
7. A. Bundulis, I.A. Shuklov, V.V. Kim, A. Mardini, J. Grube, J. Alnis, A.A. Lizunova, V.F. Razumov, R.A. Ganeev, Nanomater. **11**, 3351 (2021)
8. D.D. Torres, S. Pamidighantam, P.K. Jain, J. Phys. Chem. C **124**, 10344–10352 (2020)
9. C. Livache, B. Martinez, N. Goubet, C. Gréboval, J. Qu, A. Chu, S. Royer, S. Ithurria, M.G. Silly, B. Dubertret, E. Lhuillier, Nat. Commun. **10**, 2125 (2019)
10. V. Grigel, L.K. Sagar, K. De Nolf, Q. Zhao, A. Vantomme, J. De Roo, I. Infante, Z. Hens, Chem. Mater. **30**, 7637–7647 (2018)
11. M. Green, H. Mirzai, J. Mater. Chem. C **6**, 5097–5112 (2018)
12. E. Lhuillier, M. Scarafagio, P. Hease, B. Nadal, H. Aubin, X.Z. Xu, N. Lequeux, G. Patriarche, S. Ithurria, B. Dubertret, Nano Lett. **16**, 1282–1286 (2016)
13. R.A. Ganeev, G.S. Boltaev, V.V. Kim, K. Zhang, A.I. Zvyagin, M.S. Smirnov, O.V. Ovchinnikov, P.V. Redkin, M. Wöstmann, H. Zacharias, C. Guo, Opt. Express **26**, 35013–35025 (2018)
14. R.A. Ganeev, I.A. Shuklov, A.I. Zvyagin, D.V. Dyomkin, M.S. Smirnov, O.V. Ovchinnikov, A.A. Lizunova, A.M. Perepukhov, V.S. Popov, V.F. Razumov, Opt. Express **29**, 16710–16726 (2021)
15. M. Sheik-Bahae, A.A. Said, T.H. Wei, D.J. Hagan, E.W. Van Stryland, IEEE J. Quantum Electron. **26**, 760–769 (1990)
16. S. Srivastava, N.A. Kotov, Accounts Chem. Res. **41**, 1831–1841 (2008)
17. Z. Deng, K.S. Jeong, P. Guyot-Sionnest, ACS Nano **8**, 11707–11714 (2014)
18. R.A. Ganeev, M. Suzuki, M. Baba, M. Ichihara, H. Kuroda, J. Phys. B **41**, 045603 (2008)
19. H. Singhal, P.A. Naik, M. Kumar, J.A. Chakera, P.D. Gupta, J. Appl. Phys. **115**, 033104 (2014)
20. Y. Fu, R.A. Ganeev, G.S. Boltaev, S.K. Maurya, V.V. Kim, C. Zhao, A. Rout, C. Guo, Nanophot. **8**, 849–858 (2019)
21. R.A. Ganeev, Photonics **9**, 757 (2022)
22. C. Vozzi, M. Nisoli, J.-P. Caumes, G. Sansone, S. Stagira, S. De Silvestri, M. Vecchiocattivi, D. Bassi, M. Pascolini, L. Poletto, P. Villoresi, G. Tondello, Appl. Phys. Lett. **86**, 111121 (2005)
23. H. Ruf, C. Handschin, R. Cireasa, N. Thiré, A. Ferré, S. Petit, D. Descamps, E. Mével, E. Constant, V. Blanchet, B. Fabre, Y. Mairesse, Phys. Rev. Lett. **110**, 083902 (2013)
24. G.S. Boltaev, V.V. Kim, V.S. Yalishev, M. Iqbal, N.A. Abbasi, R.A. Ganeev, A.S. Alnaser, Photonics **7**, 66 (2020)
25. G.S. Boltaev, R.A. Ganeev, V.V. Kim, N.A. Abbasi, M. Iqbal, A.S. Alnaser, Opt. Express **28**, 18859–18875 (2020)
26. M. Lewenstein, P. Balcou, M.Y. Ivanov, A. L'Huillier, P.B. Corkum, Phys. Rev. A **49**, 2117 (1994)
27. R.A. Ganeev, G.S. Boltaev, V.V. Kim, M. Venkatesh, A.I. Zvyagin, M.S. Smirnov, O.V. Ovchinnikov, M. Wöstmann, H. Zacharias, C. Guo, J. Appl. Phys. **126**, 193103 (2019)

Terms and Conditions

Springer Nature journal content, brought to you courtesy of Springer Nature Customer Service Center GmbH ("Springer Nature").

Springer Nature supports a reasonable amount of sharing of research papers by authors, subscribers and authorised users ("Users"), for small-scale personal, non-commercial use provided that all copyright, trade and service marks and other proprietary notices are maintained. By accessing, sharing, receiving or otherwise using the Springer Nature journal content you agree to these terms of use ("Terms"). For these purposes, Springer Nature considers academic use (by researchers and students) to be non-commercial.

These Terms are supplementary and will apply in addition to any applicable website terms and conditions, a relevant site licence or a personal subscription. These Terms will prevail over any conflict or ambiguity with regards to the relevant terms, a site licence or a personal subscription (to the extent of the conflict or ambiguity only). For Creative Commons-licensed articles, the terms of the Creative Commons license used will apply.

We collect and use personal data to provide access to the Springer Nature journal content. We may also use these personal data internally within ResearchGate and Springer Nature and as agreed share it, in an anonymised way, for purposes of tracking, analysis and reporting. We will not otherwise disclose your personal data outside the ResearchGate or the Springer Nature group of companies unless we have your permission as detailed in the Privacy Policy.

While Users may use the Springer Nature journal content for small scale, personal non-commercial use, it is important to note that Users may not:

1. use such content for the purpose of providing other users with access on a regular or large scale basis or as a means to circumvent access control;

2. use such content where to do so would be considered a criminal or statutory offence in any jurisdiction, or gives rise to civil liability, or is otherwise unlawful;

3. falsely or misleadingly imply or suggest endorsement, approval , sponsorship, or association unless explicitly agreed to by Springer Nature in writing;

4. use bots or other automated methods to access the content or redirect messages

5. override any security feature or exclusionary protocol; or

6. share the content in order to create substitute for Springer Nature products or services or a systematic database of Springer Nature journal content.

In line with the restriction against commercial use, Springer Nature does not permit the creation of a product or service that creates revenue, royalties, rent or income from our content or its inclusion as part of a paid for service or for other commercial gain. Springer Nature journal content cannot be used for inter-library loans and librarians may not upload Springer Nature journal content on a large scale into their, or any other, institutional repository.

These terms of use are reviewed regularly and may be amended at any time. Springer Nature is not obligated to publish any information or content on this website and may remove it or features or functionality at our sole discretion, at any time with or without notice. Springer Nature may revoke this licence to you at any time and remove access to any copies of the Springer Nature journal content which have been saved.

To the fullest extent permitted by law, Springer Nature makes no warranties, representations or guarantees to Users, either express or implied with respect to the Springer nature journal content and all parties disclaim and waive any implied warranties or warranties imposed by law, including merchantability or fitness for any particular purpose.

Please note that these rights do not automatically extend to content, data or other material published by Springer Nature that may be licensed from third parties.

If you would like to use or distribute our Springer Nature journal content to a wider audience or on a regular basis or in any other manner not expressly permitted by these Terms, please contact Springer Nature at

onlineservice@springernature.com